Journal of proteome research

pubs.acs.org/jpr

Article

Plasma TNFRSF11B as a New Predictive Inflammatory Marker of Sepsis−ARDS with Endothelial Dysfunction

Dong Zhang,[§] Changjuan Xu,[§] Jintao Zhang, Rong Zeng, Qian Qi, Jiawei Xu, Yun Pan, Xiaofei Liu, Shuochuan Shi, Jianning Zhang,* and Liang Dong*

Cite This: https://doi.org/10.1021/acs.jproteome.3c00576

Read Online

ACCESS | Metrics & More | Article Recommendations | Supporting Information

ABSTRACT: Inflammation plays an important role in the development of sepsis−acute respiratory distress syndrome (ARDS). Olink inflammation-related biomarker panels were used to analyze the levels of 92 inflammation-related proteins in plasma with sepsis−ARDS (n = 25) and healthy subjects (n = 25). There were significant differences in 64 inflammatory factors, including TNFRSF11B in sepsis−ARDS, which was significantly higher than that in controls. Functional analysis showed that TNFRSF11B was closely focused on signal transduction, immune response, and inflammatory response. The TNFRSF11B level in sepsis−ARDS plasma, LPS-induced mice, and LPS-stimulated HUVECs significantly increased. The highest plasma concentration of TNFRSF11B in patients with sepsis−ARDS was 10−20 ng/mL, and 10 ng/mL was selected to stimulate HUVECs. Western blot results demonstrated that the levels of syndecan−1, claudin−5, VE−cadherin, occludin, aquaporin−1, and caveolin−1 in TNFRSF11B-stimulated HUVECs decreased, whereas that of connexin-43 increased in TNFRSF11B-stimulated HUVECs. To the best of the authors' knowledge, this study was the first to reveal elevated TNFRSF11B in sepsis−ARDS associated with vascular endothelial dysfunction. In summary, TNFRSF11B may be a new potential predictive and diagnostic biomarker for vascular endothelium damage in sepsis−ARDS.

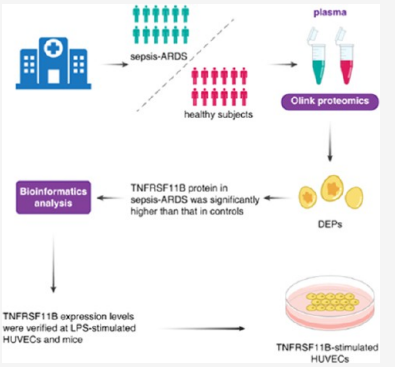

KEYWORDS: *TNFRSF11B, sepsis−ARDS, endothelial dysfunction, glycocalyx, junctions*

INTRODUCTION

Acute respiratory distress syndrome (ARDS) is a progressive and destructive disease caused by various intra- or extrapulmonary factors, and its treatment and rehabilitation are relatively difficult. The main features of ARDS include vascular endothelium injury, inflammatory cell aggregation, and mesenchymal edema.[1] Vascular endothelium plays an important role in inflammatory cell aggregation and pulmonary interstitial edema.[2,3] Endothelial permeability includes trans- and paracellular permeability. Glycocalyx, a negatively charged gelatinous substance, is the first barrier between endothelium and blood, containing more heparan sulfate and syndecan-1 (SDC-1).[4] Glycocalyx damage leads to dysfunction of transcellular and paracellular permeability, which results in permeable change, leukocyte adhesion, and blood flow disorder.[5]

Transcellular permeability is mainly achieved by caveolae-mediated transcellular transport. Caveolae accounted for 15% of the endothelium volume and 95% of cell surface vesicles. Caveolin-1 is the surface marker protein of caveolae, and it is necessary for maintaining the structure and function of caveolae.[6] Zhu et al. showed that glycocalyx suppressed caveolin-1-dependent endothelial transcytosis to improve blood−brain barrier integrity in ischemic stroke.[7] Aquaporins (AQPs) are hydrophobic proteins that regulate the water balance of pulmonary vessels in physiological or pathological states. AQPs include 1−5, among which AQP-1 is mainly distributed in pulmonary microvascular endothelium.[8] Down-regulation of AQP-1 expression leads to aggravation of edema, whereas upregulation of AQP-1 expression alleviates acute pulmonary edema.[9] Chen et al. demonstrated that gold nanoparticle-mediated AQP-1 induction is dependent on caveolin-1, but it requires the repression of ERK activity.[10]

Intercellular transport mediated by tight, adherent, and gap junctions is the main mechanism for endothelial intercellular permeability. Occludin, claudin-5, and zonula occludens 1 (ZO-1) are the key components of a tight junction; the down-regulation of the tight-junction protein regulated inflammatory signal transduction and lung endothelial permeability during lung injury.[11,12] VE-cadherin, a core component of the adherent junction, plays an important role in endothelial permeability.[13] Zhu et al. demonstrated that inflammatory mediator interleukin-1β disrupted VE-cadherin localization in the cell surface to impair endothelial stability.[14] In addition, studies have shown

Received: September 7, 2023

that the connexin-43 (CX-43) protein elevation of gap junctions in ARDS endothelium exacerbated lung vascular permeability.[15,16]

Tumor necrosis factor (TNF) receptor superfamily 11B (TNFRSF11B, TNFRSF11B is also called OPG), a member of the TNF receptor superfamily, is originally known to participate in bone homeostasis and found to play an important role in lung diseases.[17] Miyake et al. found that knockout of TNFRSF11B reduced airway inflammation in mouse models of asthma.[18] To et al. found that TNFRSF11B was related to the severity or progression of COPD and could be used as a potential biomarker of COPD.[19] Kemperman et al. showed that the level of plasma TNFRSF11B was higher in patients with sepsis and septic shock than in those without sepsis.[20] Patients with high TNFRSF11B concentrations at intensive care unit (ICU) admission had a higher risk of dying within 30 days than patients with low TNFRSF11B concentrations.[20] However, the level and role of TNFRSF11B in patients with sepsis−ARDS remain unclear.

This study aimed to identify whether TNFRSF11B is a potential predictive and diagnostic biomarker for sepsis−ARDS with endothelial dysfunction by exploring the level of TNFRSF11B in patients with sepsis−ARDS and its function of transcellular and paracellular permeability in human umbilical vein endothelial cells (HUVECs).

MATERIALS AND METHODS

Materials

Lipopolysaccharide (LPS, *Escherichia coli* 055:B5) was purchased from Sigma−Aldrich (St. Louis, MO). Anti-SDC-1 (ET1703−42), anticaveolin-1 (ET1603−1), anti-AQP-1 (ET1703−34), antioccludin (R1510−33), anticlaudin-5 (ET1703−58), and anticonnexin-43 (HA721312), anti-GAPDH (ET1601−4), HRP-conjugated goat antimouse IgG (HA1006), and HRP-conjugated goat antirabbit IgG (HA1001) were obtained from HUABIO (Zhejiang, China). The BCA protein assay kit (PC0020) and anti-ZO-1 (K001718P) were purchased from Solarbio (Beijing, China). Anti-TNFRSF11B (sc-390518) was obtained from Santa Cruz Biotechnology (Dallas). TNFRSF11B ELISA kits of human (EK0480) and mouse (EK0481) were supplied by Boster (Wuhan, China).

Human Subjects

Patients with sepsis-induced ARDS (n = 25) and control subjects (n = 25) in this study from the Shandong Provincial Qianfoshan Hospital were enrolled. Table 1 shows the clinical characteristics of patients. Those with sepsis−ARDS were diagnosed on the basis of the diagnostic criteria for sepsis revised by the European Society of Intensive Care Medicine and the Society of Critical Care Medicine in 2016 and the Berlin definition used to diagnose ARDS in 2012.[21,22] The control subjects came to the physical examination center, and they were ruled out of inflammation-related diseases. Blood samples were taken from all patients after obtaining informed consent. Every individual had approximately 3 mL of peripheral venous blood taken and placed into a sterile tube. Subsequently, the plasma was extracted at 1000g for 30 min and stored in a −80 °C refrigerator. This study was approved by the First Affiliated Hospital of Shandong First Medical University & Shandong Provincial Qianfoshan Hospital ethics committee [2023 (S423)].

Table 1. Baseline Characteristics Stratified by Sepsis−ARDS Patients and Normal Status[1]

characteristic	normal	sepsis−ARDS
number	25	25
T (°C)	36.3 [36.1−36.4]	38.2 [36.6−38.8]
HR (times/min)	72.0 [64.0−79.5]	110.0 [94.0−120.5]
RR (times/min)	16.0 [15.5−17.0]	26.0 [20.0−31.0]
SBP (mmHG)	131.0 [119.0−137.5]	96.0 [75.0−104.5]
WBC (10*9/L)	6.40 [5.40−7.20]	15.66 [12.42−22.02]
PCT (ng/mL)	<0.04	9.55 [0.87−128.11]
P/F (mmHG)	>300	160.00 [90.85−225.30]
plasma albumin (g/L)	43.2 [41.9−45.6]	27.5 [23.1−33.5]
D-dimer (mg/L)	0.20 [0.15−0.46]	6.33 [2.42−18.45]
LAC (mmol/L)	NA	5.3 [2.6−10.9]
IL-6 (pg/mL)	2.38 [1.22−3.94]	89.68 [32.34−858.20]
CD3 + T cells (%)	69.05 [62.31−73.36]	67.89 [51.56−76.36]
CD3 + CD4 + T cells (%)	39.34 [31.93−44.88]	42.01 [26.92−51.95]
CD3 + CD8 + T cells (%)	24.12 [19.30−31.15]	21.66 [10.61−28.79]
CD4 + T/CD8 + T	1.66 [1.22−2.23]	1.64 [1.19−2.96]
CD19 + B cells (%)	12.08 [8.30−19.88]	20.65 [12.55−36.48]
CD16 + CD56 + NK cells	18.61 [11.18−22.80]	9.20 [4.91−17.31]
CRP (mg/L)	<3.34	136.00 [85.86−249.43]
platelets (10*9/L)	216 [197−248]	50 [27−114]

[1]Data are expressed as the median (interquartile range). HR, heart rate; RR, respiratory rate; SBP, systolic blood pressure; WBC, white blood cell; P/F, PaO2/FiO2; LAC, lactic acid; CRP, C-reactive protein; NA, not available.

Olink Inflammation-Related Biomarker Analysis

Plasma samples from sepsis−ARDS (n = 25) and control subjects (n = 25) were evaluated using the Olink inflammation panels, which allow for simultaneous analysis of 92 inflammation-related biomarkers. In summary, the target protein binds with great specificity to the double-oligonucleotide-labeled antibody probe, and the oligonucleotide sequence is quantified via microfluidic real-time PCR amplification.

Bioinformatics Analysis

The differentially expressed proteins (DEPs) were assigned to each Gene Ontology (GO) and Kyoto Encyclopedia of Genes and Genomes (KEGG) database term or pathway. Subsequently, the findings of the enrichment analysis were compared on the basis of the setting of DEPs in the Olink inflammatory panel. In addition, Spearman's correlation analysis was used to explore the correlation between TNFRSF11B and DEPs. Protein−protein interactions (PPI) were used to visualize the network of TNFRSF11B with DEPs.

Animal Grouping

Male C57BL/6 mice (six/group, 7−8 weeks old, weighing 18−20 g; Jinan Pengyue Animal Feeding Co., Ltd.) were randomly divided into LPS and control groups. All mice were housed at the Animal Experiment Center of the Shandong Provincial Qianfoshan Hospital. The LPS group was injected intraperitoneally with LPS (20 mg/kg) to stimulate the cells for 6 h. The control group was injected intraperitoneally with the same amount of normal saline. Mouse lungs were isolated for TNFRSF11B detection. Mouse blood was centrifuged at 4 °C 1000g for 20 min, and the supernatant was used to detect the TNFRSF11B level.

Histopathology

Lung sections (5 μm thickness) were stained with hematoxylin and eosin (HE) after dewaxing and dehydration. The lung injury

https://doi.org/10.1021/acs.jproteome.3c00576
J. Proteome Res. XXXX, XXX, XXX−XXX

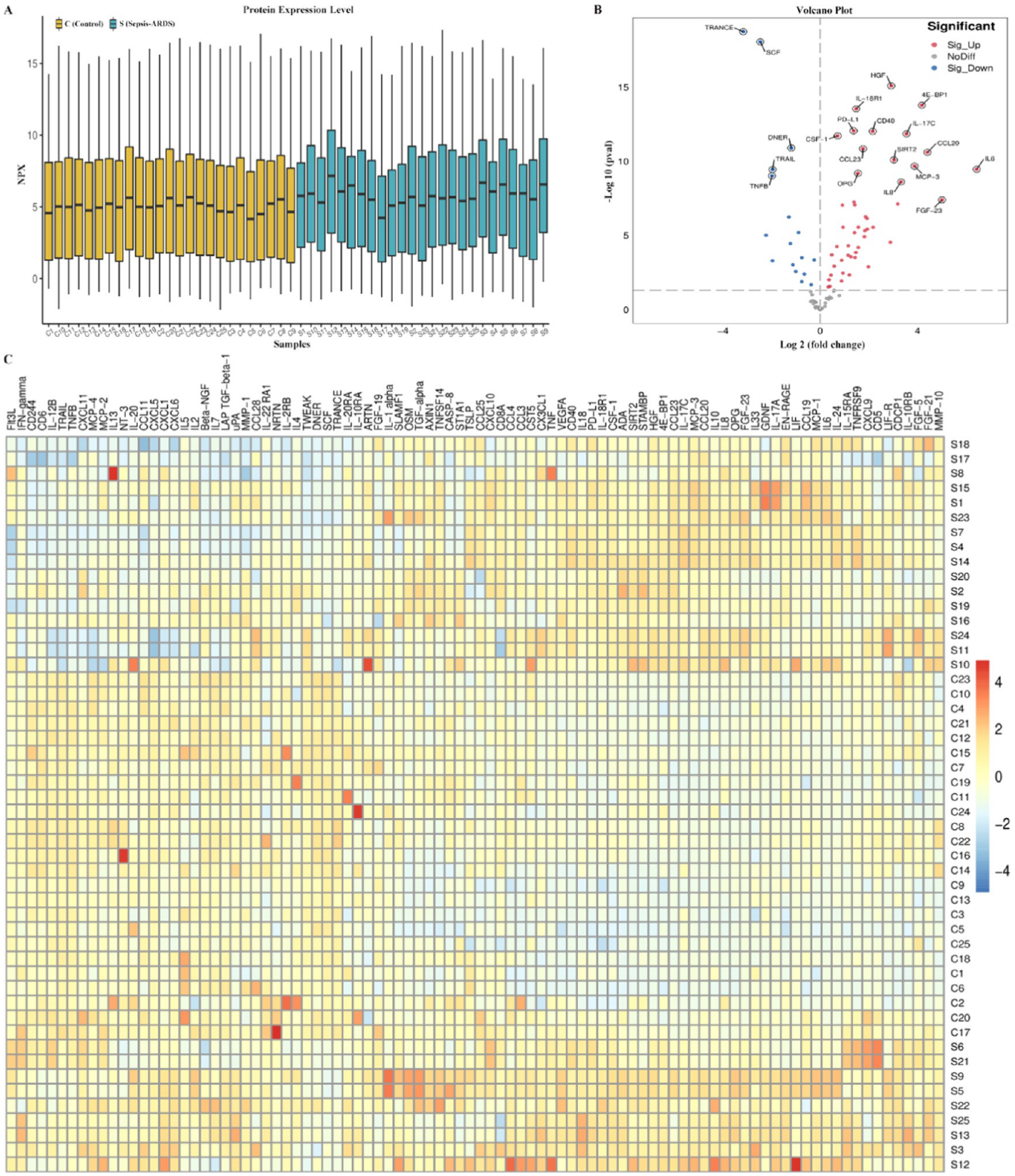

Figure 1. All DEPs in inflammation-related biomarkers between the sepsis−ARDS and control groups. (A) Protein expression in the sepsis−ARDS (n = 25) and control groups (n = 25). (B) Volcanic visualization of DEPs based on 92 inflammation-related biomarkers, including OPG (TNFRSF11B) in sepsis−ARDS, was significantly higher than that in controls. (C) Heatmap of 92 inflammation-related proteins.

evaluation was consistent with the previous description criteria, which mainly included alveolar hyperemia, infiltration of inflammatory cells into the alveolar wall, and alveolar wall thickening.[15]

Cell Culturing

The HUVECs were obtained from Shanghai Zhong Qiao Xin Zhou Biotechnology Co., Ltd. and cultured in complete culture medium (10% fetal bovine plasma, 100 U/mL penicillin, and 0.1

https://doi.org/10.1021/acs.jproteome.3c00576
J. Proteome Res. XXXX, XXX, XXX−XXX

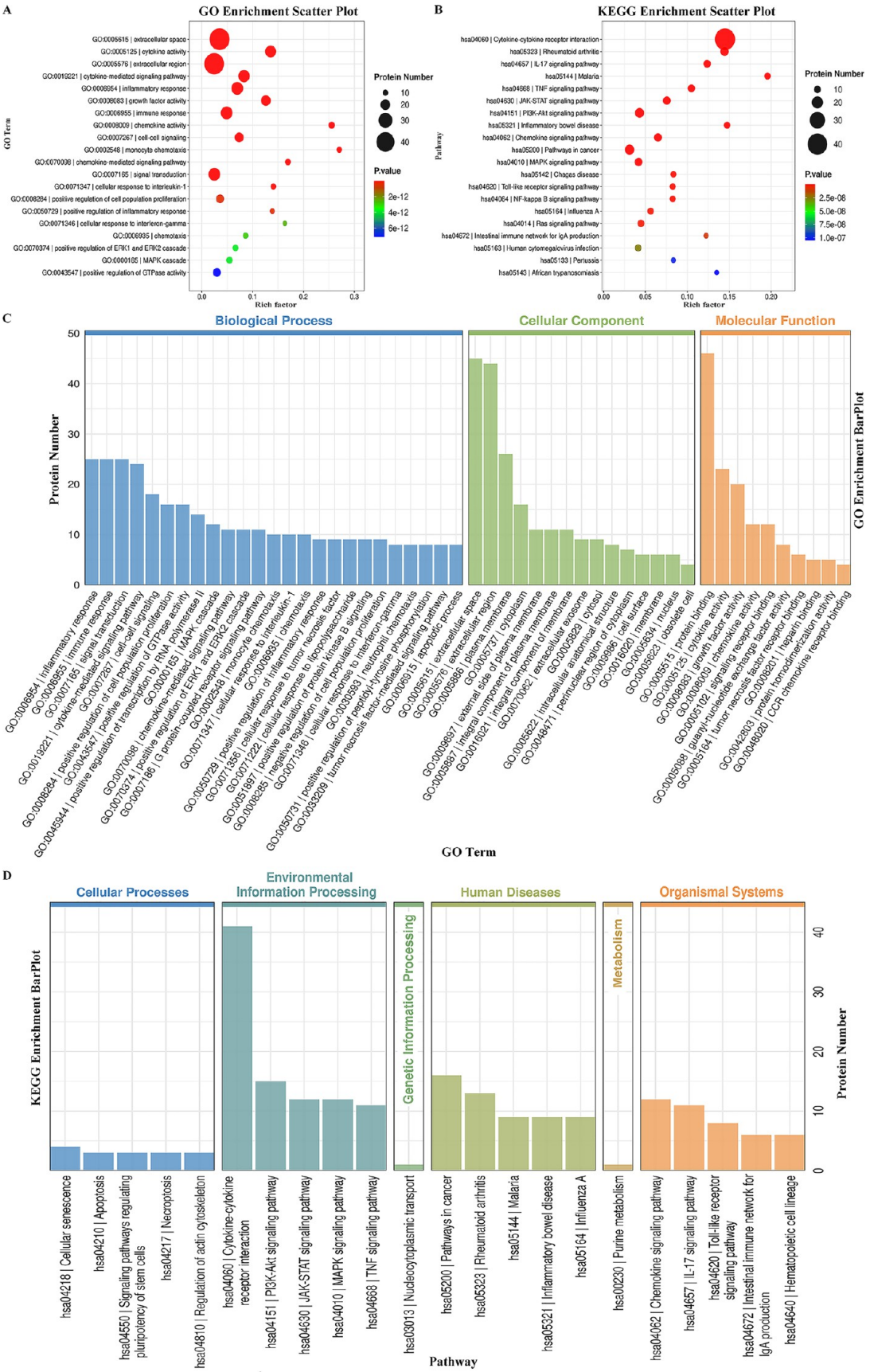

Figure 2. GO and KEGG enrichment analyses of DEPs. (A) GO enrichment analysis with a scatter plot based on the background of 92 inflammation-related proteins. (B) KEGG enrichment analysis with a scatter plot based on the background of 92 inflammation-related proteins. (C) GO enrichment analysis with a bar plot based on the background of 92 inflammation-related proteins. (D) KEGG enrichment bar plot analysis with a bar plot based on the background of 92 inflammation-related proteins.

https://doi.org/10.1021/acs.jproteome.3c00576
J. Proteome Res. XXXX, XXX, XXX−XXX

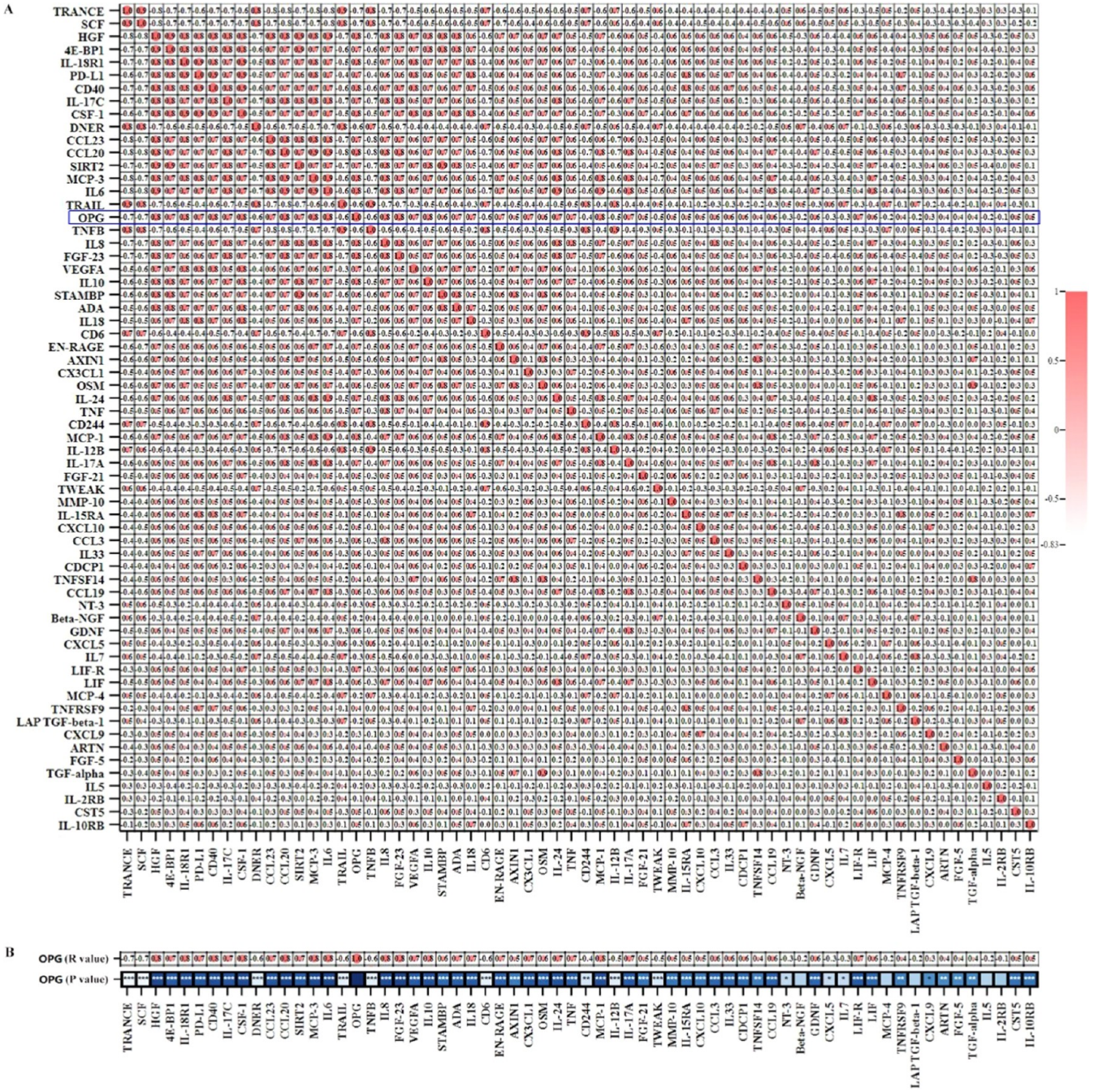

Figure 3. (A) Correlative analysis between DEPs in sepsis−ARDS and control groups. (B) Visualization of the correlation between OPG (TNFRSF11B) and DEPs. *$p < 0.05$, **$p < 0.01$, ***$p < 0.001$, ****$p < 0.0001$. NS, not significant.

mg/mL streptomycin) in an incubator with a humidified atmosphere of 95% air and 5% CO_2 at 37 °C.

The HUVECs were further divided into control and LPS groups for detecting TNFRSF11B. The control group was cultured in a culture medium without treatment, whereas the LPS group was treated with LPS (1 μg/mL) for 6 h stimulation. Then, the cells and cell supernatant were used for detecting TNFRSF11B.

The HUVECs were further divided into TNFRSF11B and control groups for detecting the TNFRSF11B function. The TNFRSF11B group was treated with TNFRSF11B (10 ng/mL) for 6 h stimulation. Finally, HUVECs were used for the detection of occludin, claudin-5, VE-cadherin, SDC-1, connexin-43, ZO-1, caveolin-1, and AQP-1.

Western Blot Analysis

The HUVECs or lungs were lysed in ice-cold RIPA buffer containing protease inhibitors, and the protein concentrations were measured with a BCA protein assay kit. The protein samples in 10% separation gel were electrophoresed and transferred onto PVDF membranes. The PVDF membranes were incubated with 5% nonfat milk at room temperature for 1 h and then incubated with primary antibody (anti-SDC-1, anticaveolin-1, anti-AQP-1, anti-ZO-1, antioccludin, anticlaudin-5, anticonnexin-43, anti-VE-cadherin, anti-TNFRSF11B, and anti-GAPDH) overnight. On the following day, the PVDF

https://doi.org/10.1021/acs.jproteome.3c00576
J. Proteome Res. XXXX, XXX, XXX−XXX

A

ProteinA	GeneA	ProteinB	GeneB	Score Threshold
9606.ENSP00000225831	CCL2	9606.ENSP00000297350	TNFRSF11B	536
9606.ENSP00000237837	FGF23	9606.ENSP00000297350	TNFRSF11B	681
9606.ENSP00000241261	TNFSF10	9606.ENSP00000297350	TNFRSF11B	820
9606.ENSP00000263851	IL7	9606.ENSP00000297350	TNFRSF11B	451

B

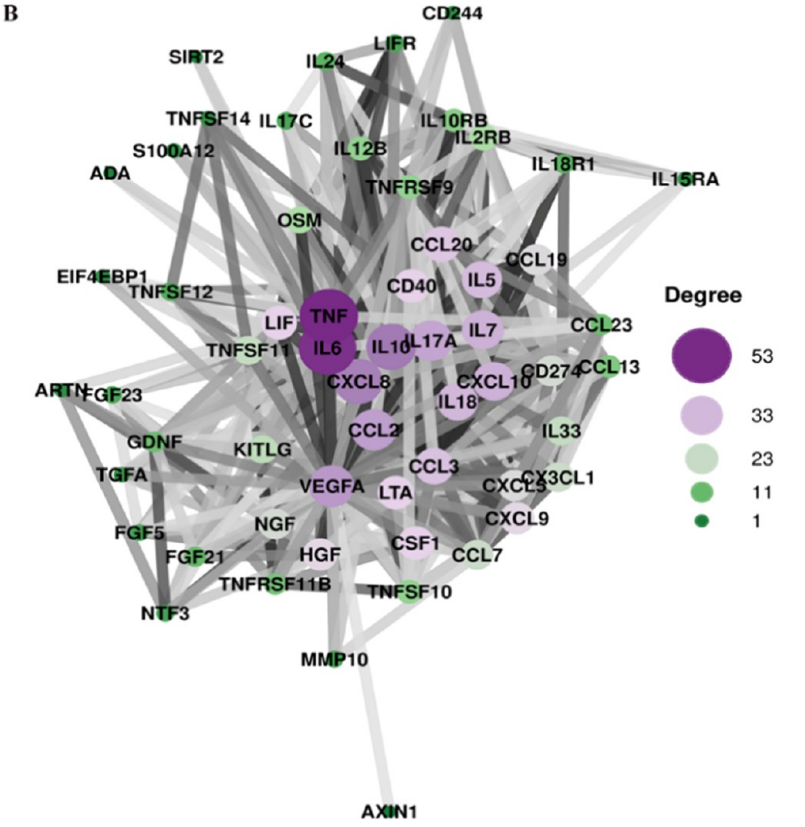

Figure 4. (A) PPI network analysis between TNFRSF11B and CCL2, FGF23, TNFSF10, and IL7. (B) Visualization of the PPI network analysis of DEPs.

membranes were washed three times with TBST and incubated at room temperature with HRP-conjugated goat antimouse IgG or HRP-conjugated goat antirabbit IgG for 1.5 h. Finally, enhanced chemiluminescence was used to detect protein bands, and the intensities of the bands were quantified by using ImageJ.

mRNA Sequencing

The treated and pretreated HUVEC cells and lungs were stored in a refrigerator at −80 °C. The HUVEC cells and lungs were extracted and purified, and sample libraries were constructed. The sample library was sequenced using the Illumina Hiseq sequencing platform by Shanghai Bioatlas Technology Co., Ltd. (Shanghai, China).

Statistical Analysis

Statistical analysis was completed on GraphPad Prism version 9.0. The results are expressed as the means ± standard deviation (SD). A *t*-test or Mann−Whitney *U* test was used to evaluate the statistical significance in the two groups. The Spearman rank correlation test was used to analyze the correlation of TNFRSF11B. The cutoff level of plasma TNFRSF11B was determined by the area under the curve (AUC) analysis of receiver operating characteristics (ROCs). $p < 0.05$ was considered statistically significant.

RESULTS

Elevated TNFRSF11B in Olink Inflammation-Related Biomarker Analysis

The characteristics of patients with or without sepsis−ARDS are displayed in Table 1. The Olink inflammation-related biomarker technology was used to evaluate the expression levels of inflammation-related proteins (n = 92) between sepsis−ARDS and control groups. Figure 1A shows the protein expression levels in all human plasma samples. A total of 64 different proteins were identified between the sepsis−ARDS and control groups, including 47 proteins with upregulated expression and 17 proteins with downregulated expression in the sepsis−ARDS group, among which TNFRSF11B was significantly elevated (Figure 1B). Figure 1C shows a heatmap containing differentially expressed inflammation-related proteins.

Functional Enrichment Analysis of DEPs

GO and KEGG enrichment analyses based on the background of 92 inflammation-related proteins were performed to investigate the potential effects of DEPs. The results showed that these protein functions focus on signal transduction, immune response, and inflammatory response and that these functions may be related to the cytokine−cytokine receptor interaction and MAPK and TNF signaling pathways (Figure 2A−D). In addition, correlation analyses between proteins were performed

https://doi.org/10.1021/acs.jproteome.3c00576
J. Proteome Res. XXXX, XXX, XXX−XXX

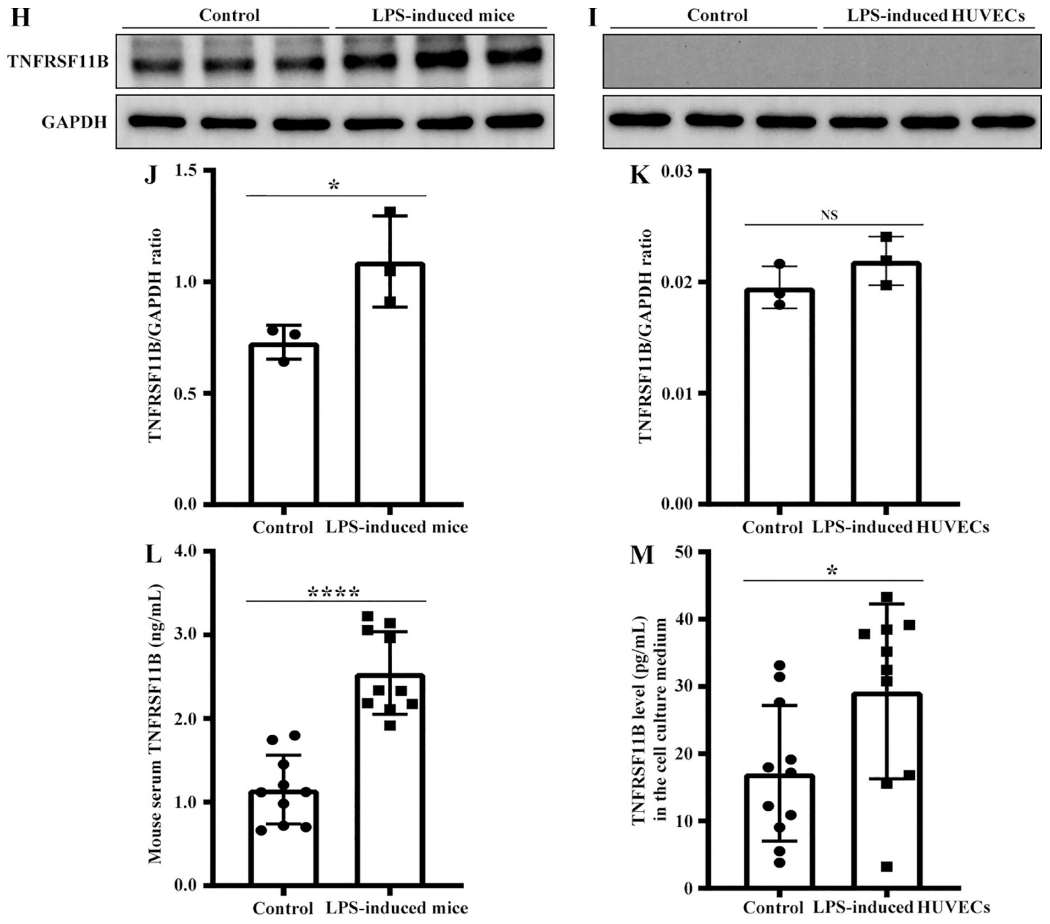

Figure 5. Validation of TNFRSF11B in human sepsis−ARDS serum, LPS-induced mice, and LPS-stimulated HUVECs. (A) Olink data visualization of TNFRSF11B. (B) Receiver operating characteristic (ROC) curve of serum TNFRSF11B in sepsis−ARDS and control groups. (C) Validation of TNFRSF11B concentration in sepsis−ARDS and control groups. (D) ROC curve of TNFRSF11B concentration in sepsis−ARDS and control groups. (E) Lung injury was evaluated by HE staining. (F) mRNA level of TNFRSF11B in LPS-induced ARDS mice. (G) mRNA level of TNFRSF11B in LPS-stimulated HUVECs. (H) Protein level of TNFRSF11B in LPS-induced ARDS mice. (I) Protein level of TNFRSF11B in LPS-stimulated HUVECs. (J) TNFRSF11B intensity in LPS-induced ARDS mice. (K) TNFRSF11B intensity in LPS-stimulated HUVECs. (L) TNFRSF11B concentration of serum in LPS-induced ARDS mice. (M) TNFRSF11B concentration of cell culture medium in LPS-stimulated HUVECs. Data are expressed as the means ± SD of three independent experiments. *$p < 0.05$, **$p < 0.01$, ***$p < 0.001$, ****$p < 0.0001$. NS, not significant.

to explore the interactions between the different proteins. As shown in Figure 3, IL18R1, CCL20, MCP-1, MCP-3, IL-6, IL-8, and IL-10 were significantly positively correlated with TNFRSF11B, whereas TNFRSF11B was significantly negatively correlated with SCF, TNFB, DNER, and CD6. In addition, TNFSF10 had a higher degree score in the PPI network, suggesting that it may play an important role in sepsis−ARDS (Figure 4A,B).

Elevated TNFRSF11B in Human Sepsis−ARDS Plasma, LPS-Induced Mice, and LPS-Stimulated HUVECs

Figure 5A shows the level distribution of TNFRSF11B on the basis of the expression of the Olink inflammation related biomarkers. The AUC of TNFRSF11B was 0.9792 (95% CI: 0.9465−1.000, $P < 0.0001$) according to the ROC curve analysis that was based on the TNFRSF11B level in human sepsis−ARDS plasma (Figure 5B). The optimal cutoff value based on the Youden index was 0.88, with sensitivity and specificity of 0.88 and 1, respectively. TNFRSF11B was selected as a new potential predictive biomarker for ARDS for further validation, combined with the above results. The ELISA results showed that the TNFRSF11B level in the plasma of the sepsis−ARDS group was significantly higher than that in the control group, consistent with the trend observed in Olink data (Figure 5C). The AUC of TNFRSF11B was 0.9600 (95% CI: 0.9149−1.000, $P < 0.0001$) according to the ROC curve analysis that was based on the TNFRSF11B concentration in human sepsis−ARDS plasma (Figure 5D). The optimal cutoff value based on the Youden index was 0.76, with sensitivity and specificity of 0.88 and 0.88, respectively. HE results showed that alveolar hyperemia, infiltration of inflammatory cells into the alveolar wall, and alveolar wall thickening in LPS-induced mice were more serious than the control group (Figure 5E). The mRNA level of TNFRSF11B in LPS-stimulated mice or HUVECs increased (Figure 5F,G). The protein level of TNFRSF11B in LPS-stimulated mice increased, whereas that in LPS-stimulated HUVECs did not (Figure 5H−5K). The level of TNFRSF11B in LPS-stimulated mouse plasma or LPS-stimulated HUVECs culture medium increased (Figure 5L,5M).

Validation of TNFRSF11B Function by TNFRSF11B-Stimulated HUVECs

The highest concentration of TNFRSF11B in sepsis−ARDS plasma was found to be 10−20 ng/mL by ELISA (Figure 5). Therefore, HUVECs were treated with TNFRSF11B (10 ng/mL) for stimulation for 6 h. The proteins occludin, claudin-5,

https://doi.org/10.1021/acs.jproteome.3c00576
J. Proteome Res. XXXX, XXX, XXX−XXX

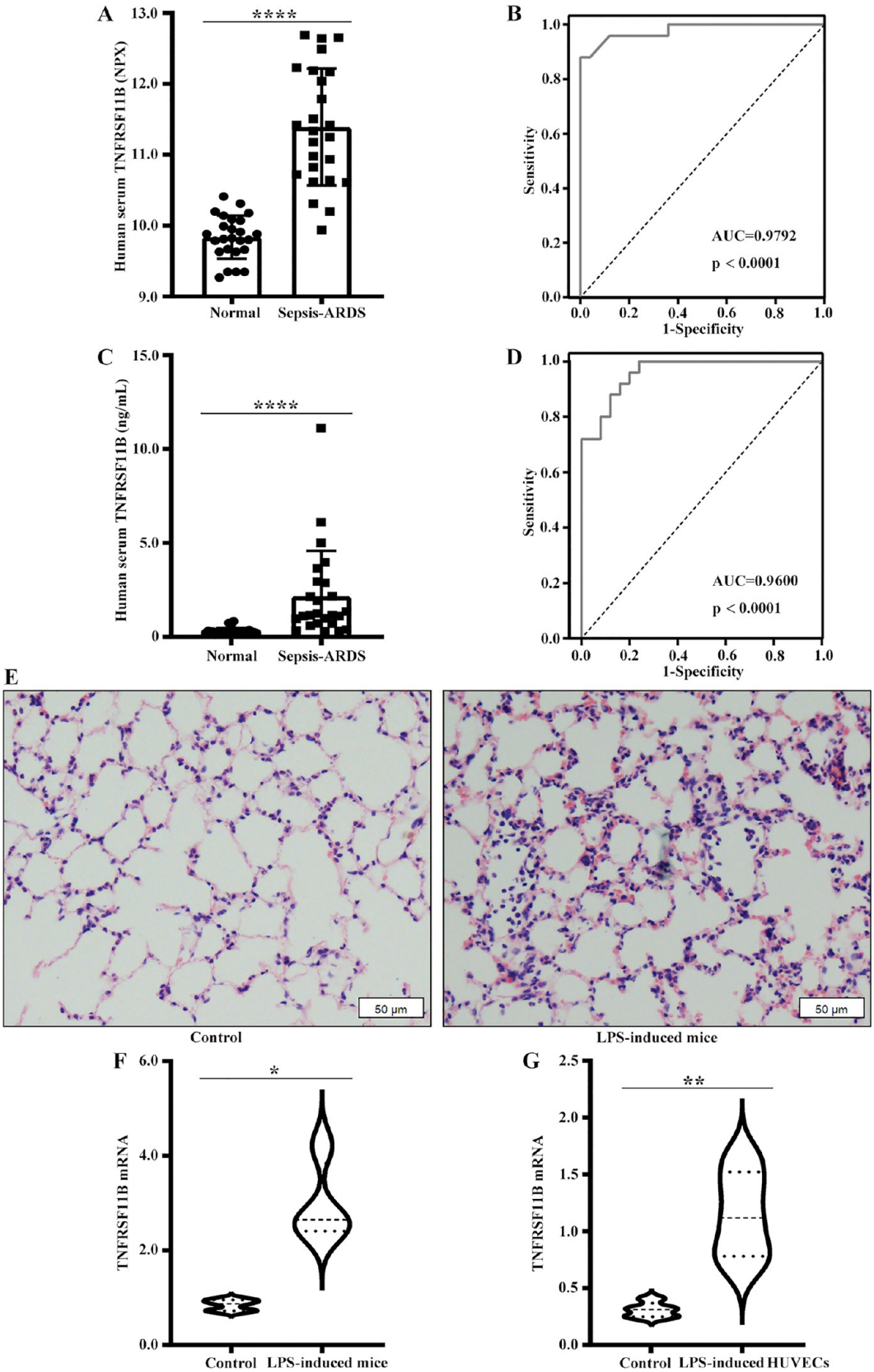

VE-cadherin, SDC-1, connexin-43, ZO-1, caveolin-1, and AQP-1 were used to evaluate the role of TNFRSF11B in HUVECs. The Western blot results demonstrated that occludin, claudin-5, VE-cadherin, SDC-1, caveolin-1, and AQP-1 decreased significantly, connexin-43 increased significantly, and ZO-1 did not increase significantly after TNFRSF11B stimulation (Figure 6). These results indicated that TNFRSF11B caused serious damage to the vascular endothelium of glycocalyx, caveolae transport, and tight, adherent, and gap junctions in patients with sepsis−ARDS, and thus aggravated pulmonary edema.

https://doi.org/10.1021/acs.jproteome.3c00576
J. Proteome Res. XXXX, XXX, XXX−XXX

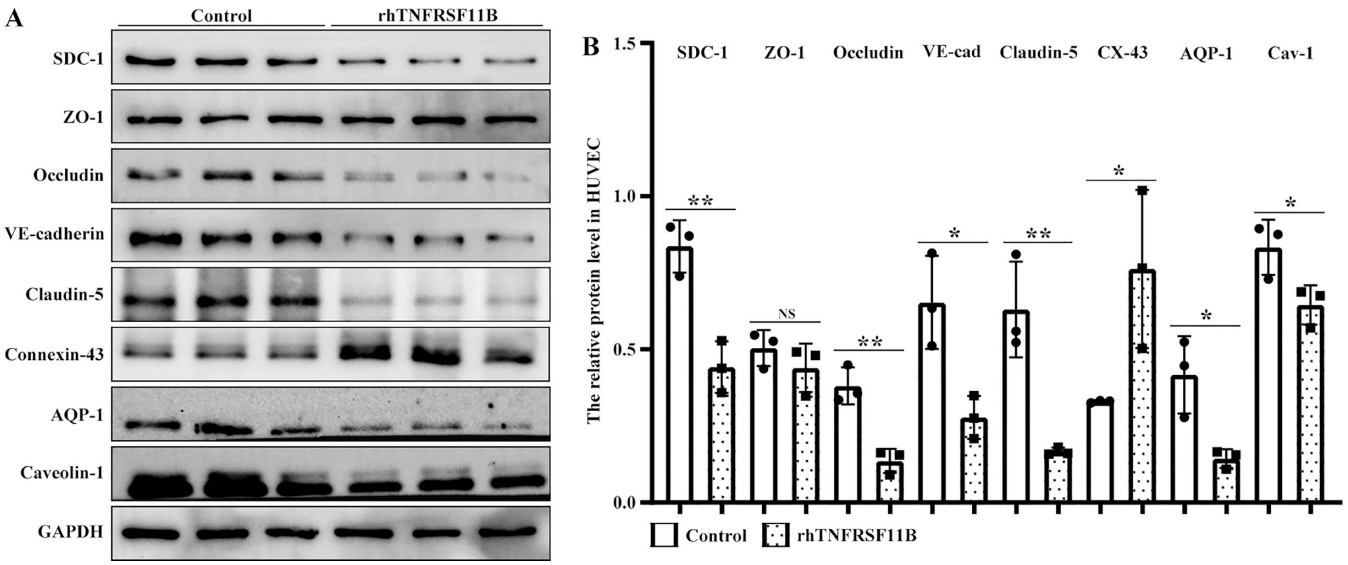

Figure 6. Validation of the TNFRSF11B function in HUVECs. (A) Western blot detection of occludin, claudin-5, VE-cadherin, SDC-1, Cav-1, and AQP-1, CX-43, and ZO-1 proteins. (B) Relative protein intensity in TNFRSF11B-stimulated HUVECs. Data are expressed as the means ± SD of three independent experiments. *$p < 0.05$, **$p < 0.01$. NS, not significant.

DISCUSSION

The endothelial structural injury by inflammatory cytokines is the main pathological feature of sepsis-induced ARDS. The Olink proteomics can identify inflammatory biomarkers associated with sepsis-induced ARDS subjects. This study showed that the level of plasma TNFRSF11B with sepsis-induced ARDS increased. Moreover, TNFRSF11B significantly aggravated the endothelial barrier damage.

TNFRSF11B binds to TNFSF11 and inhibits TNFSF11/TNFRSF11A signaling in bone resorption and homeostasis.[23] TNFRSF11B was recently revealed to be engaged in the immune system and vascular biology, both of which are involved in the pathophysiology of sepsis.[24] Zauli et al. suggested that a pathological increase in plasma TNFRSF11B may play an important role in promoting leukocyte or endothelial cell adhesion.[25] Shimamura et al. implied that a high plasma TNFRSF11B level is associated with unfavorable outcomes in ischemic stroke.[26] Wen et al. showed plasma TNFRSF11B as a potential mechanism of endothelial dysfunction in patients with obstructive sleep apnea.[27] However, the role of TNFRSF11B in sepsis-induced ARDS remains to be understood. In the present study, plasma TNFRSF11B in patients with sepsis-induced ARDS was found to be elevated, and TNFRSF11B induced the HUVEC dysfunction of glycocalyx and transcellular and paracellular permeability. Hence, a high expression of TNFRSF11B in sepsis-induced ADRS could be considered a negative predictor.

TNFSF11 binds to TNFRSF11A to activate the NF-κB signaling pathway, and NF-κB is a key transcription factor in inflammatory signaling.[28] Gregorczyk et al. reported that TNFRSF11B effectively blocked the TNFSF11/TNFRSF11A system and reduced airway inflammation.[29] However, Miyake et al. uncovered that OPG deficiency by gene knockout in asthmatic mice relieves the inflammatory response.[18] In this study, TNFSF11 was found to be significantly decreased in patients with sepsis−ARDS, whereas TNFRSF11B significantly increased. However, the mRNA level of TNFSF11 was not changed in LPS-induced mice or HUVECs than in the control (data not shown). These results might imply that TNFRSF11B, as a pathogenic inflammatory factor, led to the impairment of HUVEC function through a certain signaling pathway.

SDC-1, as an important component of glycocalyx, operated as a physical barrier on endothelium, preventing solutes from readily moving through the transcellular and paracellular space.[30] Our previous research showed that protecting the glycocalyx greatly reduced tight-junction damage in LPS-induced ARDS.[31] Mensah et al. demonstrated that glycocalyx degradation disrupted endothelium gap junction CX-43, blocking the molecular transport that maintains endothelium homeostasis.[32] Zhu et al. demonstrated that glycocalyx suppressed caveolin-1-dependent endothelial transcytosis for improving blood−brain barrier integrity in ischemic stroke.[7] Siddiqui et al. showed that caveolin-1 is necessary for adherent junction assembly or maintenance.[33] The present study results showed that TNFRSF11B can reduce the expression of occludin, claudin-5, VE-cadherin, caveolin-1, and SDC-1 and increase that of connexin-43, which may be one of the reasons why TNFRSF11B can aggravate LPS-induced ARDS.

With in-depth studies on TNFRSF11B, TNF-related apoptosis-inducing ligands, SDC-1 and glycosaminoglycans, regulate the biological functions of TNFRSF11B.[34−37] Benslimane-Ahmin et al. revealed that the proangiogenic properties of TNFRSF11B are mediated by the proteoglycan SDC-1.[38] Standal et al. study showed that TNFRSF11B binding to SDC-1 on the surface of myeloma cells may remove TNFRSF11B from the osteoblast−osteoclast interface, where TNFRSF11B plays a major role.[35] Standal et al. in a study also showed that soluble SDC-1 does not affect TNFRSF11B activity by using Chinese hamster ovary cells transfected with TNFRSF11A and stimulated with soluble TNFSF11.[35] The results of this study support the idea that TNFRSF11B induces SDC-1 shedding, but the shedding of SDC-1 does not affect the signaling of TTNFRSF11B binding with SDC-1 on the surface of cells and then leads to cell permeability damage.

Water channel obstruction is one of the important mechanisms leading to pulmonary edema in lung injury.[39] AQP-1 is a subtype of the AQPs family that drives water through the membrane barrier in the lungs.[40] ARDS is associated with

https://doi.org/10.1021/acs.jproteome.3c00576
J. Proteome Res. XXXX, XXX, XXX−XXX

decreased AQP-1 protein expression, decreased ability to clear pulmonary edema, and increased pulmonary vascular permeability. The present study results showed that TNFRSF11B can reduce AQP-1 expression in HUVECs and then adjust water channel transportation.

This study has some limitations. The Olink test is relatively expensive, and the sepsis−ARDS (n = 25) and normal (n = 25) subjects were included in accordance with the inclusion and exclusion diagnostic criteria due to economic reasons.

CONCLUSIONS

TNFRSF11B seriously affects the vascular endothelial function of sepsis−ARDS. Adding TNFRSF11B to the clinical model could significantly improve the prediction ability in patients with sepsis−ARDS.

ASSOCIATED CONTENT

Data Availability Statement

The raw data of *Mus musculus* and HUVECs mRNA sequencing were deposited to NCBI under the BioProject ID: PRJNA930203 and PRJNA1018893, respectively. Any additional information required to reanalyze the data reported in this paper is available from the lead contact upon request.

Supporting Information

The Supporting Information is available free of charge at https://pubs.acs.org/doi/10.1021/acs.jproteome.3c00576.

Information of 92 inflammation-related proteins in Olink analysis (Table S1) (PDF)

Raw data of the Olink proteomics analysis (XLSX)

AUTHOR INFORMATION

Corresponding Authors

Jianning Zhang − *Department of Respiratory and Intensive Care Unit, The First Affiliated Hospital of Shandong First Medical University and Shandong Provincial Qianfoshan Hospital, Shandong Institute of Respiratory Diseases, Shandong Characteristic Laboratory of Clinical Transformation of Respiratory Biological Immunity and Regenerative Medicine, Jinan 250021 Shandong, China*; Email: icuzjn@163.com

Liang Dong − *Department of Respiratory and Intensive Care Unit, Shandong Provincial Qianfoshan Hospital, Shandong University, Jinan 250021 Shandong, China; Department of Respiratory and Intensive Care Unit, The First Affiliated Hospital of Shandong First Medical University and Shandong Provincial Qianfoshan Hospital, Shandong Institute of Respiratory Diseases, Shandong Characteristic Laboratory of Clinical Transformation of Respiratory Biological Immunity and Regenerative Medicine, Jinan 250021 Shandong, China*; Email: dl5506@126.com

Authors

Dong Zhang − *Department of Respiratory and Intensive Care Unit, Shandong Provincial Qianfoshan Hospital, Shandong University, Jinan 250021 Shandong, China*; orcid.org/0000-0001-7323-7699

Changjuan Xu − *Department of Respiratory and Intensive Care Unit, The First Affiliated Hospital of Shandong First Medical University and Shandong Provincial Qianfoshan Hospital, Shandong Institute of Respiratory Diseases, Shandong Characteristic Laboratory of Clinical Transformation of Respiratory Biological Immunity and Regenerative Medicine, Jinan 250021 Shandong, China*

Jintao Zhang − *Department of Respiratory and Intensive Care Unit, The First Affiliated Hospital of Shandong First Medical University and Shandong Provincial Qianfoshan Hospital, Shandong Institute of Respiratory Diseases, Shandong Characteristic Laboratory of Clinical Transformation of Respiratory Biological Immunity and Regenerative Medicine, Jinan 250021 Shandong, China*

Rong Zeng − *Department of Respiratory and Intensive Care Unit, Shandong Provincial Qianfoshan Hospital, Shandong University, Jinan 250021 Shandong, China*

Qian Qi − *Department of Respiratory and Intensive Care Unit, The First Affiliated Hospital of Shandong First Medical University and Shandong Provincial Qianfoshan Hospital, Shandong Institute of Respiratory Diseases, Shandong Characteristic Laboratory of Clinical Transformation of Respiratory Biological Immunity and Regenerative Medicine, Jinan 250021 Shandong, China*

Jiawei Xu − *Department of Respiratory and Intensive Care Unit, The First Affiliated Hospital of Shandong First Medical University and Shandong Provincial Qianfoshan Hospital, Shandong Institute of Respiratory Diseases, Shandong Characteristic Laboratory of Clinical Transformation of Respiratory Biological Immunity and Regenerative Medicine, Jinan 250021 Shandong, China*

Yun Pan − *Department of Respiratory and Intensive Care Unit, Shandong Provincial Qianfoshan Hospital, Shandong University, Jinan 250021 Shandong, China*

Xiaofei Liu − *Department of Respiratory and Intensive Care Unit, The First Affiliated Hospital of Shandong First Medical University and Shandong Provincial Qianfoshan Hospital, Shandong Institute of Respiratory Diseases, Shandong Characteristic Laboratory of Clinical Transformation of Respiratory Biological Immunity and Regenerative Medicine, Jinan 250021 Shandong, China*

Shuochuan Shi − *Department of Respiratory and Intensive Care Unit, The First Affiliated Hospital of Shandong First Medical University and Shandong Provincial Qianfoshan Hospital, Shandong Institute of Respiratory Diseases, Shandong Characteristic Laboratory of Clinical Transformation of Respiratory Biological Immunity and Regenerative Medicine, Jinan 250021 Shandong, China*

Complete contact information is available at: https://pubs.acs.org/10.1021/acs.jproteome.3c00576

Author Contributions

[§]D.Z. and C.X. contributed equally to this work. D.Z. and J.Z. designed the study. D.Z., R.Z., Q.Q., and J.X. collected the human samples and the clinical information. D.Z., Y.P., X.L., and S.S. performed the animal and cell experiments and analyzed the data. D.Z., J.Z., and L.D. wrote and revised the article. All authors have read and approved the final article.

Funding

This work was supported by the National Natural Science Foundation of China (Grant Nos. 82270032 and 82100056), the Key Research and Development Program of Shandong Province (Grant No. 2021SFGC0504), the Shandong Provincial Natural Science Foundation (Grant Nos. ZR2021LSW015 and ZR2021QH170), and the Jinan Clinical Medicine Research Program for Respiratory Disease (Grant No. 202132002).

Notes

The authors declare no competing financial interest.

■ ACKNOWLEDGMENTS

The authors wish to thank Shanghai Bioprofile Technology Company Ltd. for technical support in the mRNA sequence analysis.

■ ABBREVIATIONS

TNFRSF11B, tumor necrosis factor receptor superfamily 11B; ARDS, acute respiratory distress syndrome; AUC, area under the curve; ROC, receiver operating characteristic; HUVEC, human umbilical vein endothelial cell; SDC-1, syndecan-1; AQP, aquaporin; ZO-1, zonula occludens 1; CX-43, connexin-43; Cav-1, caveolin-1; VE-cad, VE-cadherin

■ REFERENCES

(1) Zhou, Y.; Li, P.; Goodwin, A. J.; Cook, J. A.; Halushka, P. V.; Chang, E.; et al. Exosomes from endothelial progenitor cells improve outcomes of the lipopolysaccharide-induced acute lung injury. *Crit. Care* **2019**, *23* (1), No. 44, DOI: 10.1186/s13054-019-2339-3.

(2) Caudrillier, A.; Kessenbrock, K.; Gilliss, B. M.; Nguyen, J. X.; Marques, M. B.; Monestier, M.; et al. Platelets induce neutrophil extracellular traps in transfusion-related acute lung injury. *J. Clin. Invest.* **2012**, *122* (7), 2661−2671.

(3) Simmons, S.; Erfinanda, L.; Bartz, C.; Kuebler, W. M. Novel mechanisms regulating endothelial barrier function in the pulmonary microcirculation. *J. Physiol.* **2019**, *597* (4), 997−1021.

(4) LaRivière, W. B.; Schmidt, E. P.The pulmonary endothelial glycocalyx in ARDS: a critical role for heparan sulfate. In *Current Topics in Membranes*; Elsevier, 2018; Vol. *82*, pp 33−52.

(5) Wautier, J. L.; Wautier, M. P. Vascular permeability in diseases. *Int. J. Mol. Sci.* **2022**, *23* (7), No. 3645, DOI: 10.3390/ijms23073645.

(6) Hiromura, M.; Nohtomi, K.; Mori, Y.; Kataoka, H.; Sugano, M.; Ohnuma, K.; et al. Caveolin-1, a binding protein of CD26, is essential for the anti-inflammatory effects of dipeptidyl peptidase-4 inhibitors on human and mouse macrophages. *Biochem. Biophys. Res. Commun.* **2018**, *495* (1), 223−229.

(7) Zhu, J.; Li, Z.; Ji, Z.; Wu, Y.; He, Y.; Liu, K.; et al. Glycocalyx is critical for blood-brain barrier integrity by suppressing caveolin1-dependent endothelial transcytosis following ischemic stroke. *Brain Pathol.* **2022**, *32* (1), No. e13006.

(8) Madonna, R.; Pieragostino, D.; Rossi, C.; Confalone, P.; Cicalini, I.; Minnucci, I.; et al. Simulated hyperglycemia impairs insulin signaling in endothelial cells through a hyperosmolar mechanism. *Vasc. Pharmacol.* **2020**, *130*, No. 106678.

(9) Towne, J. E.; Harrod, K. S.; Krane, C. M.; Menon, A. G. Decreased expression of aquaporin (AQP)1 and AQP5 in mouse lung after acute viral infection. *Am. J. Respir. Cell Mol. Biol.* **2000**, *22* (1), 34−44.

(10) Chen, C. Y.; Liao, P. L.; Tsai, C. H.; Chan, Y. J.; Cheng, Y. W.; Hwang, L. L.; et al. Inhaled gold nanoparticles cause cerebral edema and upregulate endothelial aquaporin 1 expression, involving caveolin 1 dependent repression of extracellular regulated protein kinase activity. *Part. Fibre Toxicol.* **2019**, *16* (1), No. 37, DOI: 10.1186/s12989-019-0324-2.

(11) Looi, K.; Kicic, A.; Noble, P. B.; Wang, K. C. W. Intrauterine growth restriction predisposes to airway inflammation without disruption of epithelial integrity in postnatal male mice. *J. Dev. Origins Health Dis.* **2021**, *12* (3), 496−504.

(12) Wiley, J. W.; Zong, Y.; Zheng, G.; Zhu, S.; Hong, S. Histone H3K9 methylation regulates chronic stress and IL-6-induced colon epithelial permeability and visceral pain. *Neurogastroenterol. Motil.* **2020**, *32* (12), No. e13941.

(13) Komarova, Y. A.; Kruse, K.; Mehta, D.; Malik, A. B. Protein interactions at endothelial junctions and signaling mechanisms regulating endothelial permeability. *Circ. Res.* **2017**, *120* (1), 179−206.

(14) Zhu, W.; London, N. R.; Gibson, C. C.; Davis, C. T.; Tong, Z.; Sorensen, L. K.; et al. Interleukin receptor activates a MYD88-ARNO-ARF6 cascade to disrupt vascular stability. *Nature* **2012**, *492* (7428), 252−255.

(15) Cai, L.; Yi, F.; Dai, Z.; Huang, X.; Zhao, Y. D.; Mirza, M. K.; et al. Loss of caveolin-1 and adiponectin induces severe inflammatory lung injury following LPS challenge through excessive oxidative/nitrative stress. *Am. J. Physiol.: Lung Cell. Mol. Physiol.* **2014**, *306* (6), L566−L573.

(16) Parthasarathi, K. Endothelial connexin43 mediates acid-induced increases in pulmonary microvascular permeability. *Am. J. Physiol.: Lung Cell. Mol. Physiol.* **2012**, *303* (1), L33−L42.

(17) Simonet, W. S.; Lacey, D. L.; Dunstan, C. R.; Kelley, M.; Chang, M. S.; Lüthy, R.; et al. Osteoprotegerin: a novel secreted protein involved in the regulation of bone density. *Cell* **1997**, *89* (2), 309−319.

(18) Miyake, T.; Miyake, T.; Morishita, R. Genetic deletion of osteoprotegerin attenuates asthma development through suppression of inflammatory response in mice. *Cell. Immunol.* **2022**, *378*, No. 104559.

(19) To, M.; Ito, K.; Ausin, P. M.; Kharitonov, S. A.; Barnes, P. J. Osteoprotegerin in sputum is a potential biomarker in COPD. *Chest* **2011**, *140* (1), 76−83.

(20) Kemperman, H.; Schrijver, I. T.; Roest, M.; Kesecioglu, J.; van Solinge, W. W.; de Lange, D. W. Osteoprotegerin is higher in sepsis than in noninfectious SIRS and predicts 30-day mortality of SIRS patients in the intensive care. *J. Appl. Lab. Med.* **2019**, *3* (4), 559−568.

(21) Singer, M.; Deutschman, C. S.; Seymour, C. W.; Shankar-Hari, M.; Annane, D.; Bauer, M.; et al. The third international consensus definitions for sepsis and septic shock (sepsis-3). *JAMA* **2016**, *315* (8), 801−810, DOI: 10.1001/jama.2016.0287.

(22) ARDS Definition Task Force; Ranieri, V. M.; Rubenfeld, G. D.; Thompson, B. T.; Ferguson, N. D.; Caldwell, E.; Fan, E.; et al. Acute respiratory distress syndrome: the berlin definition. *JAMA* **2012**, *307* (23), 2526−2533.

(23) Boyce, B. F.; Xing, L. The RANKL/RANK/OPG pathway. *Curr. Osteoporosis Rep.* **2007**, *5* (3), 98−104.

(24) Baud'huin, M.; Duplomb, L.; Teletchea, S.; Lamoureux, F.; Ruiz-Velasco, C.; Maillasson, M.; et al. Osteoprotegerin: multiple partners for multiple functions. *Cytokine Growth Factor Rev.* **2013**, *24* (5), 401−409.

(25) Zauli, G.; Corallini, F.; Bossi, F.; Fischetti, F.; Durigutto, P.; Celeghini, C.; et al. Osteoprotegerin increases leukocyte adhesion to endothelial cells both in vitro and in vivo. *Blood* **2007**, *110* (2), 536−543.

(26) Shimamura, M.; Nakagami, H.; Osako, M. K.; Kurinami, H.; Koriyama, H.; Zhengda, P.; et al. OPG/RANKL/RANK axis is a critical inflammatory signaling system in ischemic brain in mice. *Proc. Natl. Acad. Sci. U.S.A.* **2014**, *111* (22), 8191−8196.

(27) Wen, W. W.; Ning, Y.; Zhang, Q.; Yang, Y. X.; Jia, Y. F.; Sun, H. L.; et al. TNFRSF11B: a potential plasma biomarker for diagnosis of obstructive sleep apnea. *Clin. Chim. acta* **2019**, *490*, 39−45.

(28) Donovan, C. E.; Mark, D. A.; He, H. Z.; Liou, H. C.; Kobzik, L.; Wang, Y.; et al. NF-kappa B/Rel transcription factors: c-Rel promotes airway hyperresponsiveness and allergic pulmonary inflammation. *J. Immunol.* **1999**, *163* (12), 6827−6833.

(29) Gregorczyk, I.; Maślanka, T. Blockade of RANKL/RANK and NF-κB signalling pathways as novel therapeutic strategies for allergic asthma: A comparative study in a mouse model of allergic airway inflammation. *Eur. J. Pharmacol.* **2020**, *879*, No. 173129.

(30) Wang, X. Y.; Li, X. Y.; Wu, C. H.; Hao, Y.; Fu, P. H.; Mei, H. X.; et al. Protectin conjugates in tissue regeneration 1 restores lipopolysaccharide-induced pulmonary endothelial glycocalyx loss via ALX/SIRT1/NF-kappa B axis. *Respir. Res.* **2021**, *22* (1), No. 193, DOI: 10.1186/s12931-021-01793-x.

(31) Zhang, D.; Zhang, J. T.; Pan, Y.; Liu, X. F.; Xu, J. W.; Cui, W. J.; et al. Syndecan-1 shedding by matrix metalloproteinase-9 signaling regulates alveolar epithelial tight junction in lipopolysaccharide-induced early acute lung injury. *J. Inflammation Res.* **2021**, *Volume 14*, 5801−5816.

https://doi.org/10.1021/acs.jproteome.3c00576
J. Proteome Res. XXXX, XXX, XXX−XXX

(32) Mensah, S. A.; Cheng, M. J.; Homayoni, H.; Plouffe, B. D.; Coury, A. J.; Ebong, E. E. Regeneration of glycocalyx by heparan sulfate and sphingosine 1-phosphate restores inter-endothelial communication. *PLoS One* **2017**, *12* (10), No. e0186116.
(33) Siddiqui, M. R.; Komarova, Y. A.; Vogel, S. M.; Gao, X.; Bonini, M. G.; Rajasingh, J.; et al. Caveolin-1-eNOS signaling promotes p190RhoGAP-A nitration and endothelial permeability. The. *J. Cell Biol.* **2011**, *193* (5), 841−850.
(34) Emery, J. G.; McDonnell, P.; Burke, M. B.; Deen, K. C.; Lyn, S.; Silverman, C.; et al. Osteoprotegerin is a receptor for the cytotoxic ligand TRAIL. The. *J. Biol. Chem.* **1998**, *273* (23), 14363−14367.
(35) Standal, T.; Seidel, C.; Hjertner, Ø.; Plesner, T.; Sanderson, R. D.; Waage, A.; et al. Osteoprotegerin is bound, internalized, and degraded by multiple myeloma cells. *Blood* **2002**, *100* (8), 3002−3007.
(36) Théoleyre, S.; Kwan Tat, S.; Vusio, P.; Blanchard, F.; Gallagher, J.; Ricard-Blum, S.; et al. Characterization of osteoprotegerin binding to glycosaminoglycans by surface plasmon resonance: role in the interactions with receptor activator of nuclear factor kappaB ligand (RANKL) and RANK. *Biochem. Biophys. Res. Commun.* **2006**, *347* (2), 460−467.
(37) Lamoureux, F.; Picarda, G.; Garrigue-Antar, L.; Baud'huin, M.; Trichet, V.; Vidal, A.; et al. Glycosaminoglycans as potential regulators of osteoprotegerin therapeutic activity in osteosarcoma. *Cancer Res.* **2009**, *69* (2), 526−536.
(38) Benslimane-Ahmim, Z.; Poirier, F.; Delomenie, C.; Lokajczyk, A.; Grelac, F.; Galy-Fauroux, I.; et al. Mechanistic study of the proangiogenic effect of osteoprotegerin. *Angiogenesis* **2013**, *16* (3), 575−593.
(39) Moosavi, M. S.; Elham, Y. Aquaporins 1, 3 and 5 in different tumors, their expression, prognosis value and role as new therapeutic targets. *Pathol. Oncol. Res.* **2020**, *26* (2), 615−625.
(40) Wittekindt, O. H.; Dietl, P. Aquaporins in the lung. *Pflugers Archiv: Eur. J. Physiol.* **2019**, *471* (4), 519−532.

https://doi.org/10.1021/acs.jproteome.3c00576
J. Proteome Res. XXXX, XXX, XXX−XXX